Acta Biomaterialia xxx (2016) xxx–xxx

Contents lists available at ScienceDirect

Acta Biomaterialia

journal homepage: www.elsevier.com/locate/actabiomat

Full length article

Electrospun poly-L-lactide scaffold for the controlled and targeted delivery of a synthetically obtained Diclofenac prodrug to treat actinic keratosis ☆

Germano Piccirillo [a,b], Brigida Bochicchio [a], Antonietta Pepe [a], Katja Schenke-Layland [b,c,d], Svenja Hinderer [b,c,*]

[a] Dept. of Science, University of Basilicata, 85100 Potenza (PZ), Italy
[b] Dept. of Women's Health, Research Institute for Women's Health, Eberhard-Karls-University Tübingen, 72076 Tübingen, Germany
[c] Dept. of Cell and Tissue Engineering, Fraunhofer-Institute for Interfacial Engineering and Biotechnology (IGB), 70569 Stuttgart, Germany
[d] Dept. of Medicine/Cardiology, Cardiovascular Research Laboratories, David Geffen School of Medicine at UCLA, Los Angeles, CA, USA

ARTICLE INFO

Article history:
Received 29 July 2016
Received in revised form 6 October 2016
Accepted 1 November 2016
Available online xxxx

Keywords:
Diclofenac
Actinic keratosis
Electrospinning
Multiphoton imaging
FLIM

ABSTRACT

Actinic Keratosis' (AKs) are small skin lesions that are related to a prolonged sun-damage, which can develop into invasive squamous cell carcinoma (SCC) when left untreated. Effective, specific and well tolerable therapies to cure AKs are still of great interest. Diclofenac (DCF) is the current gold standard for the local treatment of AKs in terms of costs, effectiveness, side effects and tolerability. In this work, an electrospun polylactic acid (PLA) scaffold loaded with a synthetic DCF prodrug was developed and characterized. Specifically, the prodrug was successfully synthetized by binding DCF to a glycine residue via solid phase peptide synthesis (SPPS) and then incorporated in an electrospun PLA scaffold. The drug encapsulation was verified using multiphoton microscopy (MPM) and its scaffold release was spectrophotometrically monitored and confirmed with MPM. The scaffold was further characterized with scanning electron microscopy (SEM), tensile testing and contact angle measurements. Its biocompatibility was verified by performing a cell proliferation assay and compared to PLA scaffolds containing the same amount of DCF sodium salt (DCFONa). Finally, the effect of the electrospun scaffolds on human dermal fibroblasts (HDFs) morphology and metabolism was investigated by combining MPM with fluorescence lifetime imaging microscopy (FLIM). The obtained results suggest that the obtained scaffold could be suitable for the controlled and targeted delivery of the synthesized prodrug for the treatment of AKs.

Statement of Significance

Electrospun scaffolds are of growing interest as materials for a controlled drug delivery. In this work, an electrospun polylactic acid scaffold containing a synthetically obtained Diclofenac prodrug is proposed as a novel substrate for the topical treatment of actinic keratosis. A controlled drug delivery targeted to the area of interest could enhance the efficacy of the therapy and favor the healing process. The prodrug was synthesized via solid phase, employing a clean and versatile approach to obtain Diclofenac derivatives. Here, we used multiphoton microscopy to image drug encapsulation within the fibrous scaffold and fluorescence lifetime imaging microscopy to investigate Diclofenac effects and potential mechanisms of action.

1. Introduction

The medical term "actinic keratosis (AK)" identifies small skin lesions, which appear as round, rough spots between 5 mm and 1 cm in diameter. AKs are characterized as pre-cancerous or as early-stage tumors [1,2]. This pathology is also known as "solar keratosis" or "senile keratosis" because it is more common to peo-

☆ Part of the Special Issue on Extracellular Matrix Proteins and Mimics, organized by Professor Katja Schenke-Layland.

* Corresponding author at: Fraunhofer IGB Stuttgart, Department of Cell and Tissue Engineering, Nobelstr. 12, 70569 Stuttgart, Germany.
E-mail address: svenja.hinderer@igb.fraunhofer.de (S. Hinderer).

http://dx.doi.org/10.1016/j.actbio.2016.11.002
1742-7061/

ple over 50 with fair skin and is related to a prolonged sun-damage [1]. This process, also known as photoaging, leads to an accumulation of oncogenic changes [2]. Changes related to photodamage are most evident in the extracellular matrix (ECM) [3]. The accumulation of these changes leads to a pathological ECM mainly due to the degradation and fragmentation of its components such as elastic fibers [4]. As a result, the normal repair and regenerative capacity of the ECM is inhibited [4,5]. Skin ageing processes also have a significant impact on cellular mechanisms such as DNA repair, gene expression and immune response modulation [5]. AK is considered a key event in the progression from photoaged skin to the invasive squamous cell carcinoma (SCC) [2,6]. SCC affects the keratinocytes of the epidermis layer and is the second most diffused skin cancer after the basal cell carcinoma (bcc) [1,7]. However, there are many more AKs than SCCs and it is difficult to predict exactly which lesions will progress to invasive cancer [1,2]. About 15% of the men and 6% of the women in Europe are affected by AKs. The percentages rise respectively to 34% and 18% in the European population over 70 years of age [7]. Since the average life expectancy is increasing, it is predicted that even more people will be affected by AKs in the next years [1,2,7]. Although a number of treatments are already available [8–10], the development of effective, more targeted and well-tolerable therapies for the treatment of AKs is still of great interest. The first therapy approved by the Food and Drug Administration (FDA) for the topical treatment of AKs was 5-Fluorouracil in 1962 [8] followed by Imiquimod in 1997 [8], Diclofenac (DCF) in 2002 [9,10] and Ingenol Mebutate in 2012 [9]. Among them, DCF is currently the therapy of choice in terms of costs, effectiveness, side effects and tolerability [10]. DCF belongs to the class of non-steroidal anti-inflammatory drugs (NSAIDs) and is one of the most commonly used in the world [11]. It is still not clear how DCF affects AKs, but its activity seems to be related to anti-inflammatory and anti-angiogenic effects [12]. Induced apoptosis has been also proposed as a possible DCF mechanism of action in the treatment of AKs [13]. The absorption of a drug through the outermost layer of the skin, the stratum corneum (SC), is limited [14]. Thus a specific formulation of DCF commercially known as Solaraze® is needed for the treatment of AKs. This formulation is supplied with hyaluronic acid that enables DCF accumulation in the epidermis [15]. Considering these aspects, a chemical modification of DCF that enhances its permeation through the SC is of interest since it could improve its efficacy against AKs.

Over the last two decades, electrospinning has gained growing interest as a potential polymer processing technique for applications in tissue engineering [16,17] and drug delivery [18]. Electrospinning is a process that uses a high voltage source to apply a charge of a certain polarity into a polymer solution or melt, which is then accelerated toward a collector of opposite polarity. Electrospinning is an easy way to fabricate fiber-containing scaffolds with a fiber diameter in the nano- to micrometer size scale that mimic the structure and morphology of the ECM components in the skin [16,17,19]. Biodegradable and natural materials can be electrospun, and a wide range of molecules like drugs and proteins can be incorporated in the scaffolds [18]. Polylactic acid (PLA) is a biodegradable, biocompatible polymer with beneficial mechanical properties. Moreover, it is stable over a long time and its degradation proceeds through the hydrolysis of the ester linkage in the polymer's backbone resulting in a non-toxic degradation product called lactic acid [20].

In this study, we aimed to encapsulate a chemical modified and synthetically produced DCF prodrug in an electrospun PLA scaffold in order to obtain a suitable drug delivery system to locally treat AKs. A controlled and targeted drug delivery to the region of interest could reduce the undesired side-effects and enhance the efficacy of the therapy.

2. Materials and methods

2.1. Synthesis of DCF-Glycine (DCF-Gly) prodrug

All coupling reagents were purchased from Novabiochem (EMD Millipore by Merck KGaA, Darmstadt, Germany). 2-Chlorotrityl chloride resin preloaded with glycine (H-Gly-2ClTrt Resin), the solvents and DCF sodium salt (DCFONa) were purchased by Sigma Aldrich (Steinheim, Germany). DCF free acid was obtained by the dissolution of the sodium salt in water followed by acidification and extraction [21]. For the synthesis, H-Gly-2ClTrt resin (227 mg, 0.250 mmol, substitution 1.1 mmol/g, mesh 75–150) was suspended in a solvent mixture (Dimethylformamide(DMF): Dichloromethane (DCM) = 1:1, Vf = 10 mL) using a glass frittered disk sealed in glass column equipped with a faucet. The suspension was stirred (250 rpm) for 2 h using an orbital shaker. The solvent was then removed by filtration and 8 mL of a DCM:DMF = 1:1 solution containing 148 mg (0.5 mmol) of DCF, 520 mg (1 mmol) of Benzotriazol-1-yloxy-tripyrrolidino- phosphoniumhexafluorophosphate (PyBOP) and 150 mg (1 mmol) of 1-Hydroxybenzotriazole hydrate (HOBT) were added to the resin. After shaking the mixture manually for a few minutes, 175 µL (1 mmol) of N,N-Diisopropylethylamine (DIPEA) was added and the mixture was shaken (280 rpm) using an orbital shaker for 20 h. Thereafter, the solvent was removed by filtration, the resin was washed (2x10 mL DMF, 3x10 mL Methanol (MeOH), 2x10 mL DMF, 3x10 mL DCM), and the functionalized amino acid was cleaved by adding 10 mL of a mixture of acetic acid (AcOH):2,2,2-Trifluoroethanol (TFE):DCM = 1:1:8. The solution was shaken (250 rpm) employing an orbital shaker for 30 min. The cleavage mixture was then filtered, and the resin was washed with DCM (3x5 mL). The filtrates were combined and evaporated under reduced pressure to 5% of the initial volume, and 10 mL of double distilled water was then added to precipitate the desired product. The final product was lyophilized twice to remove any solvent residual, and recovered as a white fluffy powder in a final yield of 98% (86.5 mg, 0.245 mmol).

2.2. Nuclear magnetic resonance (NMR) analysis

The crude DCF-Gly was characterized by ^{1}H- and ^{13}C- nuclear magnetic resonance (NMR) analysis. The ^{1}H- and ^{13}C- NMR spectra were acquired at room temperature on an Inova 500 NMR spectrometer (Varian, Agilent technologies, Inc., Palo Alto, CA, USA), equipped with a 5 mm triple resonance probe and z-axial gradients operating at 500 MHz for ^{1}H nuclei and 125 MHz for ^{13}C nuclei. Reference peaks for ^{1}H and ^{13}C spectra were respectively set to δ 2.49 and δ 39.5 for DMSO-d_6. Two-dimensional double quantum filtered spectroscopy (DQF-COSY) spectra were collected in the phase-sensitive mode using the States method [22]. Typical data were 2048 complex data points, 32 transients and 256 increments. Shifted sine bell squared weighting and zero filling to 2 k × 2 k were applied before Fourier transform. The 2D ^{1}H-^{13}C gradient heteronuclear single quantum correlation (adiabatic version) (gHSQCAD) experiment was carried out using the pulse sequences from the Varian user library [23]. The acquired spectra were processed with ACD®/NMR Processor Academic Edition (Advanced Chemistry Development, Inc., Toronto, Canada) and are reported in the supplementary materials (Suppl. Fig. 1A–D).

2.3. Electrospun scaffolds production

All reagents and solvents were purchased from Sigma Aldrich. The electrospun scaffolds were obtained from a 15% w/v PLA (Poly(L-lactide), #93578, Mn 59.000, Sigma Aldrich) solution

Please cite this article in press as: G. Piccirillo et al., Electrospun poly-L-lactide scaffold for the controlled and targeted delivery of a synthetically obtained Diclofenac prodrug to treat actinic keratosis, Acta Biomater. (2016), http://dx.doi.org/10.1016/j.actbio.2016.11.002

(V_f = 1 mL) either containing 10 mg of the drug of interest (PLA: DCF-Gly ratio is 15:1) or none as control. 1,1,1,3,3,3-Hexafluoro-2-propanol (HFIP, T63002, Sigma Aldrich) was used as solvent. Electrospinning experiments were performed with a customized device using 17 kV, a flow rate of 4 mL/h and an 18 G needle at an electrode distance of 18 cm.

2.4. Scanning electron microscopy (SEM)

The morphology of the electrospun scaffolds was determined using a scanning electron microscope (SEM, 1530 VP, Zeiss, Jena, Germany). After platinum sputter coating, images were acquired at a distance of 8 mm from the detector, a voltage of 15 kV and different magnifications. The ImageJ® software supplied with the DiameterJ plug-in was used for fiber diameter analysis.

2.5. Drug release experiments

For the drug release experiments, the scaffolds were incubated at 37 °C in a 1X Phosphate buffer saline (PBS, Gibco™ by Life Technologies GmbH, Darmstadt, Germany) solution. Nine mg of the drug-loaded scaffolds were fully immerged in 3 mL of 1X PBS. At different time points, 800 µL of the supernatant was taken to read the absorbance (275 nm). After each measurement we returned the supernatant to the scaffold containing solution. The amount of the released drug was estimated according to a calculated calibration curve. When using the Peppas equation [24], the release is reported as percentage [25]. In this case, the absorbance of the scaffold containing solution after 24 h was assumed as final value, since no further release occurred after that time. Micro UV-cuvettes (BrandTech™ 759210, Brand™ by Thermo Scientific, Darmstadt, Germany) and a TECAN® Infinite 200 Reader were used for all the UV measurements.

2.6. Contact angle measurements

Hydrophilicity of the electrospun substrates was analyzed using contact angle measurements with an OCA 40 (DataPhysics Instruments GmbH, Filderstadt, Germany). A water drop with the volume of 2 µL was placed onto the sample and the contact angle was measured immediately after the water deposition using a video setup and the SCA20 software (DataPhysics Instruments) as previously described [26]. Final results were calculated from 16 measurements obtained from 4 different scaffold pieces for each sample.

2.7. Uniaxial tensile testing

Electrospun scaffolds were cut into 10 mm × 20 mm rectangular pieces and clamped into the uniaxial tensile testing device (Electroforce 5500, ElectroForce® Systems Group, Bose Corporation, Minnesota, USA). The exact sample dimensions were determined before each measurement and recorded with the software for further calculations of the Young's modulus (E) and the tensile strength. The scaffolds were pulled to failure by applying a stretch of 0.025 mm/s. The Young's modulus was calculated from the initial linear slope of the stress versus strain curve for each measurement. Measured values are presented as mean ± standard deviation (each group n = 3).

2.8. Cell culture and seeding

All research was carried out in compliance with the rules for investigation of human subjects, as defined in the Declaration of Helsinki. This study was carried out in accordance with the institutional guidelines and was approved by the local research Ethics Committee (F-2012-078). After informed written consent was given, skin biopsies were obtained and human dermal fibroblasts (HDFs) were isolated by enzymatic digestion as previously described [27]. Cells were cultured in Dulbecco's Modified Eagle Medium (with L-Glutamine, DMEM11965092, Gibco™, Life Technologies GmbH) supplemented with 10% fetal calf serum (FCS, PAA Laboratories, Pasching, Austria) and 1% penicillin/streptomycin (Life Technologies GmbH). Cells were cultured in an incubator at 37 °C and in a 5% CO_2 atmosphere. Cell culture medium was changed every 3 days and cells were passaged or seeded using trypsin-EDTA (15090046, PAA Laboratories) at approximately 70% confluence.

2.9. Multiphoton microscopy (MPM)

A Titan:Sapphire femtosecond laser (MaiTai XF1 Spectra Physics, USA, Santa Clara) was used to generate 2-photon excitation. An excitation wavelength of 710 nm and a laser power of 3.2 mW were employed. The spectral emission filter ranged from 425 to 509 nm. For the imaging of the drug encapsulation, punches (Ø = 12 mm) of the scaffolds were put on Ibidi® glass bottom dishes (35 mm) and carefully pressed on the bottom with a cover glass before analysis. HDFs morphology was assessed on glass bottom dishes (Ibidi®, 35 mm) with a density of 5 x 10^4 cells per dish. After 24 h, the medium was removed and 2 mL of fresh DMEM (+ 10% FCS) was added. When the cells were incubated with the drug-loaded scaffolds, punches (Ø = 28 mm) of previously sterilized (254 nm, 2 h) scaffolds were given as well. In both cases the cells were imaged after further 24 h. The laser power was in this case adjusted to 18 mW. For the mean gray value intensity (GVI) analysis, ImageJ® was used.

2.10. In vitro cytotoxicity assay

According to an ISO 10993 accredited protocol HDFs were exposed to an extract of the samples. The test was carried out as previously described [28]. In particular the electrospun scaffolds were sterilized by UV irradiation (254 nm) for 2 h. 6cm^2 of each sample were then incubated in 1 mL FCS- and antibiotic-free DMEM medium. After 24 h, seeded HDFs were exposed for further 24 h to the extracts supplied with 10% FCS. The extraction medium was removed and a tetrazolium salt ([3-(4,5-dimethylthiazol-2-yl)-5-(3-carboxymethoxyphenyl)-2-(4-sulfophenyl)-2H-tetrazolium], MTS; G3580, CellTiter 96Aqueous One Solution Cell Proliferation Assay, Promega, Mannheim, Germany) assay was performed as per the manufacturer's protocol. Briefly, 20 µL of MTS solution were added to 100 µL of culture media. After incubation for 35 min at 37 °C, the absorbance of each well was measured at 492 nm. The test was performed for a blind, a negative control (NC; DMEM + 10% FCS) and a Sodium Dodecyl Sulfate (SDS, Life Technologies GmbH, 1% in DMEM) treated positive control (PC). For analysis, the NC was set to 100%.

2.11. Fluorescence lifetime imaging microscopy (FLIM)

FLIM was performed to assess reduced (phosphorylated) nicotinamide adenine dinucleotide (NAD(P)H) using time correlated single photon counting (TCSPC) at an excitation wavelength of 710 nm and a laser power of 18 mW. FLIM data were recorded at an acquisition time of 180 s for 512 × 512 pixels with 64 time channels. The instrument response function was recorded using urea crystals (Sigma Aldrich) at an excitation wavelength of 920 nm and a laser power of 4.5 mW for 120 s. The FLIM images were calculated using the SPCImage software (Becker &Hickl GmbH, Berlin, Germany). A two exponential decay fitting model was employed at each pixel since NAD(P)H has two different lifetimes [29]. A χ^2 < 1.1 was accepted for a good fitting. A binning fac-

Please cite this article in press as: G. Piccirillo et al., Electrospun poly-L-lactide scaffold for the controlled and targeted delivery of a synthetically obtained Diclofenac prodrug to treat actinic keratosis, Acta Biomater. (2016), http://dx.doi.org/10.1016/j.actbio.2016.11.002

tor of 6 was used in the analysis. The final results were derived from 12 images obtained from 3 different dishes (4 images/dish) for each sample.

2.12. Data analysis

All the reported graphs were plotted using Microsoft™ Excel. All data are presented as mean ± standard deviation (n = 4, unless stated otherwise in the materials and methods). Statistical significance was determined by a Student's two-tailed unpaired *t*-test; $p \leqslant 0.01$ was defined as statistically significant, unless stated otherwise.

3. Results

3.1. Synthesis of a DCF prodrug via SPPS

The DCF-Gly derivative was chosen according to the predicted values for its MW (=353.20 g/mol) and log*P* (=2.78), which were estimated using Molinspiration®, making it suitable for a transdermal delivery [14]. The synthetic scheme used for the DCF-Gly synthesis is shown in Fig. 1. The desired product was obtained with a high degree of purity (99%) according to NMR analysis (Suppl. Fig. 1) and was recovered in a high yield (98%).

3.2. Production and characterization of the scaffolds

3.2.1. Electrospinning

PLA was dissolved in HFIP either alone or in presence of DCF-Gly. Various electrospinning parameters were tested and those leading to a stable Taylor cone and jet as well as to smooth and uniform fibers were then used throughout the study. The conditions were first defined for pure PLA and then adapted for the drug-loaded scaffolds.

3.2.2. SEM und fiber diameter analysis

The morphology and fiber sizes of the PLA scaffold, the drug-loaded scaffold and the scaffold after drug release (a.r.) was investigated using SEM (Fig. 2). It was possible to generate scaffolds with a random fiber orientation. In all conditions, we obtained uniform fibers with no beads (Fig. 2A–F). After drug release, morphological changes were visible; however, the fibers were still uniform and randomly oriented (Fig. 2G–I). Fiber sizes significantly increased by the incorporation of the drug (PLA: 148 ± 9 nm versus PLA + DCF-Gly: 180 ± 9 nm; p = 0.001). Despite the change in morphology, there was no significant decrease in fiber size after drug release (PLA + DCF-Gly: 180 ± 9 nm versus PLA + DCF-Gly a.r.: 170 ± 8 nm; p = 0.48).

3.2.3. Contact angle measurement

Wettability of the scaffolds was determined using contact angle measurements (Fig. 3A–B). The analysis showed that the drug-loaded scaffolds remained highly hydrophobic (PLA + DCF-Gly: 130.1 ± 8°) and no significant changes were determined when compared with the pure PLA scaffolds (PLA: 131 ± 7°).

3.2.4. Tensile tests

PLA is an elastic and electrospinnable polymer. No significant differences were observed in regards to tensile strength (PLA: 1.84 ± 0.19 MPa versus PLA + DCF-Gly: 1.91 ± 0.18 MPa; p = 0.67) and Young's modulus (PLA: 27.4 ± 9.7 MPa versus PLA + DCF-Gly: 25.4 ± 1.2 MPa; p = 0.48) when comparing the pure electrospun PLA with the drug-containing scaffold. Like the hydrophobicity, the elastic modulus and tensile strength were not influenced by the encapsulation of the DCF prodrug. The experimental curves obtained for the PLA and the PLA + DCF-Gly scaffolds are shown in Fig. 3C and D, respectively.

3.2.5. MPM analysis

MPM of the synthesized prodrug was employed for the visualization of the drug encapsulation profiting from the presence of an aromatic ring on the DCF molecule. Whereas there was no signal detectable for pure PLA scaffolds (Suppl. Fig. 2), a strong signal was obtained for the drug-loaded PLA + DCF-Gly scaffolds (Fig. 4A) demonstrating that encapsulation with electrospinning was successful. Furthermore, multiphoton laser-induced autofluorescence signals were detected from the entire scaffold. Every fiber is clearly visible, confirming that DCF-Gly is homogeneously distributed throughout the scaffold and the single fibers. After drug release, the signals significantly decreased or were absent (Fig. 4B). Only a few fibers of the scaffold could be visualized suggesting that most of the encapsulated drug had been successfully released from the scaffold after the incubation in PBS. The obtained mean gray values (Fig. 4C) were 82 ± 12 and 8.1 ± 1.1 before and after the drug release, respectively. According to these values the percentage of the not released drug was estimated to be approximately 10%.

3.2.6. Drug release experiments

After demonstrating that the drug was successfully encapsulated within the PLA fibers, the ability of the scaffold to release the drug was investigated. The absorbance at 275 nm of the PBS solution, in which the scaffold was immerged, was constantly monitored for the first 7 h (Fig. 5A). Thereafter, it was measured again after 24, 48 and 72 h. The absorbance value was constant after the first 24 h. This time was therefore set as the end point measurement, considering that no more drug will be released after that time until having a significant scaffold hydrolysis. According to a calibration curve and assuming that no loss of the drug occurs during the electrospinning process we could estimate that 89 ± 2% of the encapsulated drug was released from the scaffold after 24 h. The obtained data were also plotted in a logarithmic form (Fig. 5B) using the equation developed by Peppas et al. [24]. Peppas equation offers a simple model to study the release mechanism of incorporated molecules from polymers. According to the value obtained for the slope, which is lower than 0.45, the release undergoes a Fickian diffusion [25].

3.2.7. In vitro cytotoxicity

The biocompatibility of the modified scaffold was assessed with a MTS assay using a standardized protocol and HDFs (Fig. 6E). A material is non-cytotoxic when the proliferation is higher than

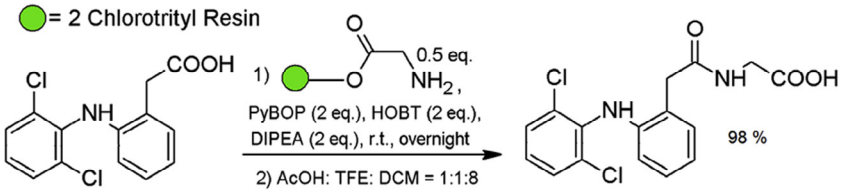

Fig. 1. Reaction scheme for the synthesis of DCF-Gly via SPPS with H-Gly-2ClTrt Resin.

Please cite this article in press as: G. Piccirillo et al., Electrospun poly-L-lactide scaffold for the controlled and targeted delivery of a synthetically obtained Diclofenac prodrug to treat actinic keratosis, Acta Biomater. (2016), http://dx.doi.org/10.1016/j.actbio.2016.11.002

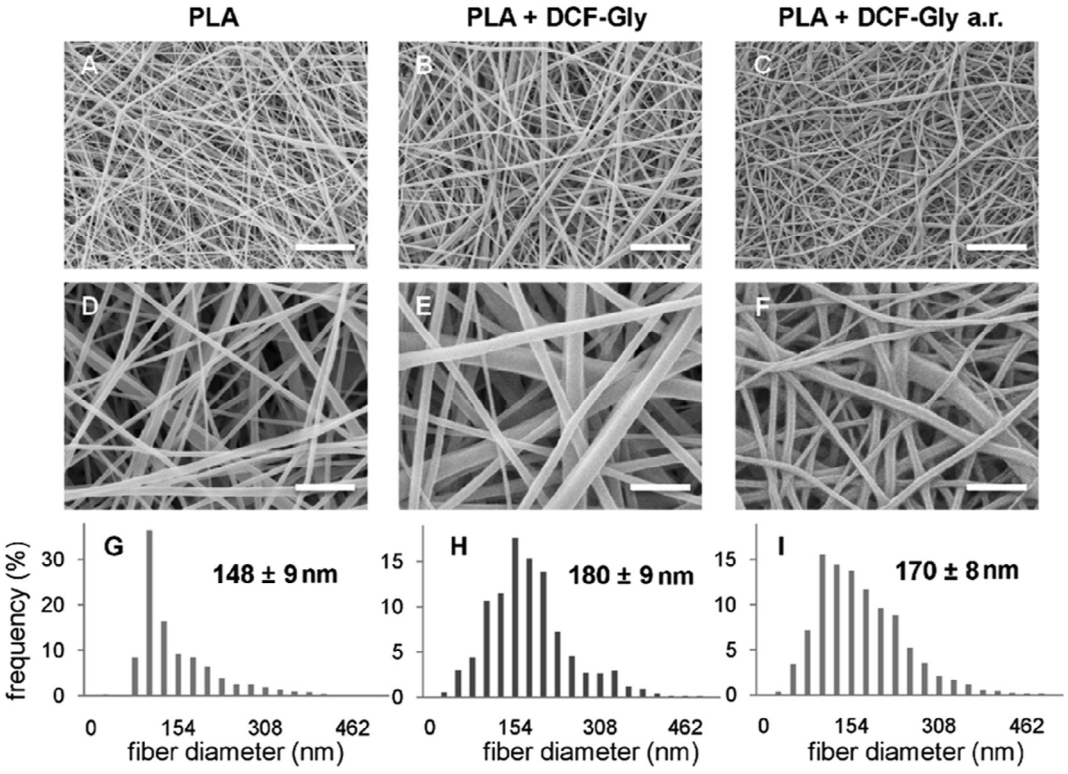

Fig. 2. Analysis of the morphology and fiber size of the electrospun scaffolds. A–F. SEM images of the electrospun scaffolds at different magnifications (a.r. = after release; scale bars: A–C = 5 μm; D–F = 1 μm). G–I: Histograms of the fiber diameter distribution and the average fiber size.

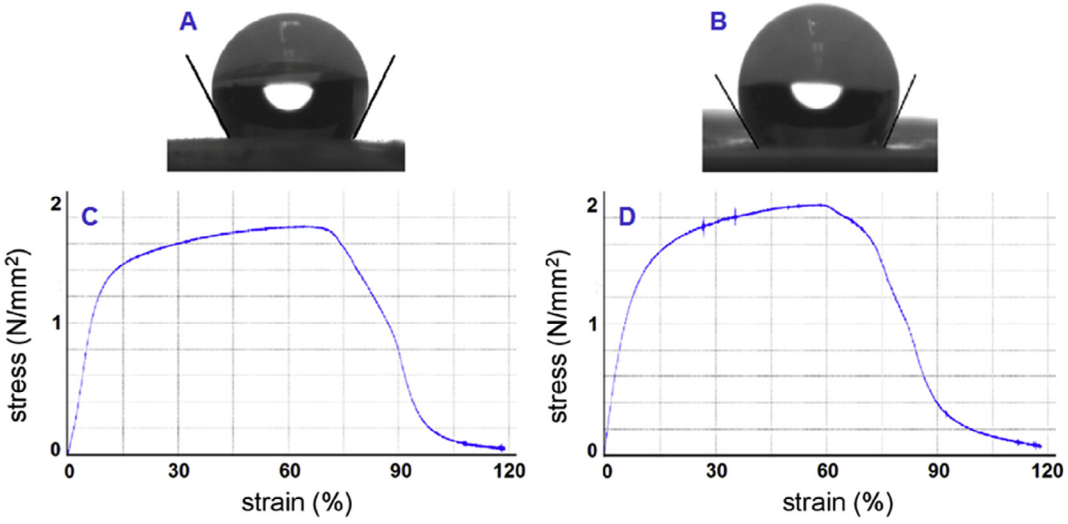

Fig. 3. Wettability assessment and mechanical testing of the electrospun scaffolds. Drop shape analysis of the pure PLA (A) and the PLA-DCF-Gly containing (B) scaffold after water deposition. Stress-Strain curves for pure PLA (C) and PLA + DCF-Gly (D).

80% relative to the NC [30]. Accordingly, we determined that the PLA scaffolds, either with or without the encapsulated DCF-Gly, showed no cytotoxic effects (cell proliferation: PLA = 104 ± 6%; PLA + DCF-Gly = 105 ± 7%). The assay was also performed with a PLA scaffold containing the non-modified DCF (DCFONa) as a positive cytotoxic control [31]. In this case, a severe cytotoxicity (cell proliferation = 16 ± 3%) was observed.

3.2.8. FLIM analysis

FLIM was performed to analyze endogenous NAD(P)H in HDFs as a measure for metabolic changes in the target cells due to the incubation together with the drug-loaded scaffolds. For FLIM analyses, a two exponential decay was employed assuming to have two different fluorescence lifetimes respectively for the free ($\tau 1$) and the protein-bound ($\tau 2$)NAD(P)H [29]. The $\alpha 1$ represents the free NAD(P)H contribution to the final lifetime values. Moreover, we aimed to correlate the obtained data directly with the results that arose from the MTS assay since the rate of tetrazolium reduction reflects the general metabolic activity/rate of glycolytic NAD(P)H [29]. No changes in the cell morphology could be observed for the DCF-Gly-loaded and non-loaded scaffolds when compared to the controls (Fig. 6A–C). The cells were elongated and showed

Please cite this article in press as: G. Piccirillo et al., Electrospun poly-L-lactide scaffold for the controlled and targeted delivery of a synthetically obtained Diclofenac prodrug to treat actinic keratosis, Acta Biomater. (2016), http://dx.doi.org/10.1016/j.actbio.2016.11.002

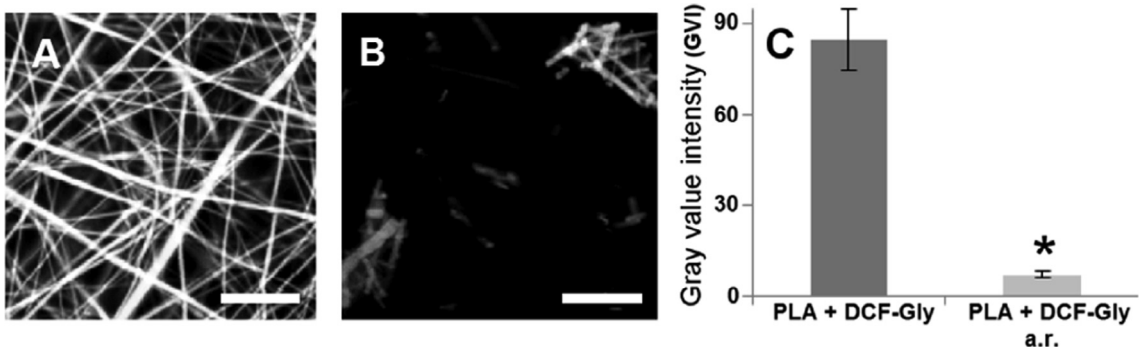

Fig. 4. MPM imaging of the DCF-Gly loaded scaffolds. MPM images (scale bar = 10 μm) of the DCF-Gly loaded scaffold before (A) and after (B) the drug release. Gray values intensities obtained from the MPM images (C).

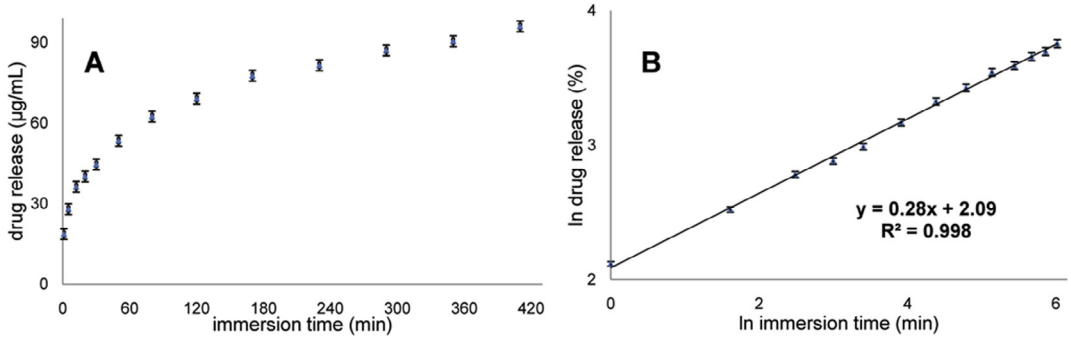

Fig. 5. Release profile of DCF-Gly from the PLA scaffold. Drug release analysis (A) and logarithmic fitting of the drug release data with Peppas equation (B). Data are presented as mean ± standard deviation (n = 4).

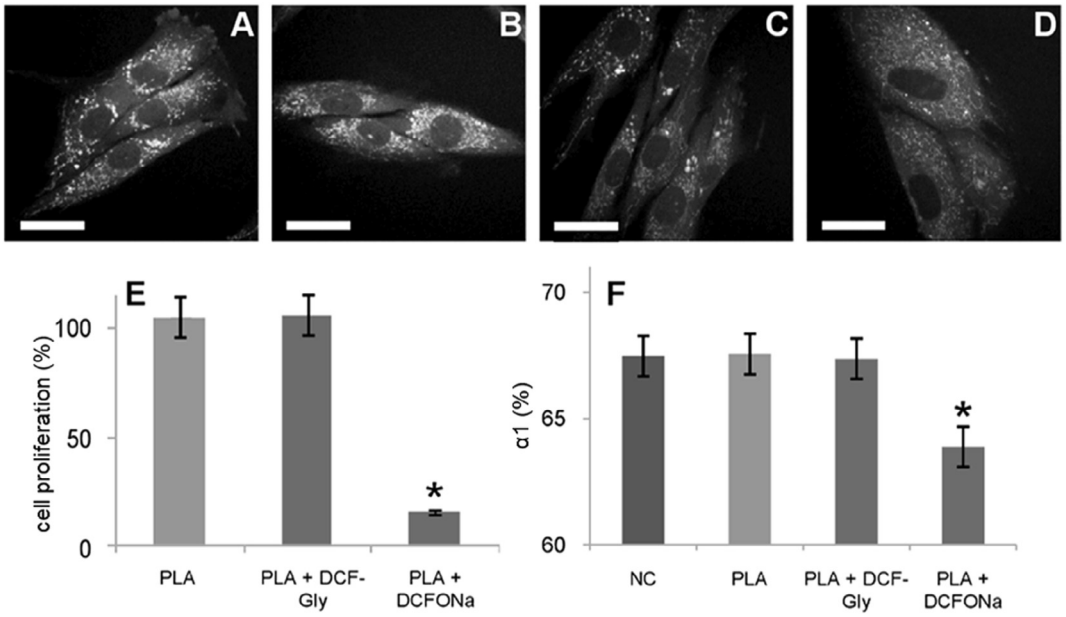

Fig. 6. Cytotoxicity assessment using HDFs. MPM images of HDFs (A–D). HDFs treated with cell culture medium only as NC (A) or in presence of PLA (B), PLA + DCF-Gly (C) and PLA + DCFONa (D) scaffolds. Scale bars equal 20 μm. Results of the accredited MTS-assay (E) and the FLIM analysis of alpha 1 using a biexponential decay (F).

the typical shape of fibroblasts [32]. However, when exposed to DCFONa, a significant morphological change was observed in the MPM images (Fig. 6D) due to induced necrosis/apoptosis [32]. Here, the cytoplasm and the nucleus were clearly altered. This morphological change correlated to a metabolic change according to the α1 values of FLIM measurements. A significant decrease in the free NAD(P)H level (α1; Fig. 6F) was observed for the PLA + DCFONa treated HDFs, but not for PLA or PLA + DCF-Gly exposed cells (PLA + DCFONa: 63.9 ± 0.9% versus NC: 67.5 ± 0.8%; p = 0.001). No significant changes in τ1and τ2 were detectable (Suppl. Fig. 3).

Please cite this article in press as: G. Piccirillo et al., Electrospun poly-L-lactide scaffold for the controlled and targeted delivery of a synthetically obtained Diclofenac prodrug to treat actinic keratosis, Acta Biomater. (2016), http://dx.doi.org/10.1016/j.actbio.2016.11.002

4. Discussion

Three-dimensional scaffolds are of growing interest among scientists for applications in the field of tissue engineering or as drug delivery systems [33,34]. Among the currently employed polymers, PLA may be the most suitable material for the production of slowly biodegradable scaffolds for biomedical applications [35]. Thus, PLA is also a suitable material to produce systems for a controlled drug delivery [36]. DCF is one of the most potent NSAIDs [37,38]. It has been used for the treatment of many different diseases such as osteoarthritis [39] and AKs [40]. Since its approval, a number of different DCF-containing products have been developed with the goal of improving efficacy, tolerability, and patient convenience [41–45]. However, no new formulations of DCF for the treatment of AKs have been proposed since its FDA approval in 2002 [9]. The DCF formulation proposed in this work should offer a new option for the local treatment of AKs. DCF has unique chemical features. For example, the amine function is a very weak base when compared to other secondary amines [46]. This feature was utilized in this study to handle DCF as an amino acid analogue in SPPS. In particular, DCF was linked to a glycine residue by forming an amidic bond to obtain a derivative (DCF-Gly) with a lower logP when compared to DCF (estimated logP: DCF-Gly = 2.78 versus DCF = 4.96). This is necessary in order to be suitable for a transdermal delivery [14]. The formation of an amidic bond is a well-used strategy for the synthesis of prodrugs since it may be easily cleaved by enzymatic hydrolysis [47,48]. Solid phase synthesis represents a clean, versatile and efficient way to avoid the use of large amounts of solvents and reagents [48]. Amide prodrugs of DCF have already been synthesized by Kumar et al. [49]. However, the synthetic scheme that was proposed in this study allowed them to reach only yields about 60% [49]. Here, we obtained a quantitative yield of 98%. Moreover, we obtained the free amino acid derivative instead of the protected ester [49], which is crucial when aiming for obtaining a proper hydrophobicity for the synthesized prodrug. For the synthesis of the DCF-Gly prodrug, a 2-Chloro Trityl Chloride (CTRL-Cl) resin was employed. The CTRL-Cl resin allows the synthesis of peptides with a carboxylic group at the C-terminus [50] and is compatible with the Fluorenyl-9-methoxycarbonyl protecting group chemistry [51,52]. Compared to the other resins, the CTRL-Cl one has not only the advantage to produce peptides free from diastereomeric side-products [50–52], but offers the possibility to operate the cleavage under mild acidic conditions (either 1% trifluoroacetic acid/DCM [51] or AcOH/TFE/DCM [52]), which is required when handling protected or modified peptides. The opportunity of binding DCF to different amino acid residues and even to longer peptide chains without the need of further purification could be employed to obtain many different DCF derivatives. This is potentially very useful considering the variety of medical applications of DCF [37–40]. The results obtained in this study by binding DCF to a glycine residue are promising since we achieved a high yield and a great degree of purity. However, the versatility of this synthesis has to be further investigated. The synthesized DCF-Gly prodrug was successfully incorporated in a PLA scaffold using electrospinning. The obtained electrospun scaffolds were then characterized in order to demonstrate that it is a suitable system for the topical treatment of AKs. In particular, the morphology of the scaffold was investigated with SEM. This technique is the often used for the investigation of nanostructures. It is reliable and allows high magnifications with a good resolution [53]. Thus this analysis was necessary to investigate the scaffold morphology, analyze the diameter distributions and compare them. The SEM investigation showed a homogeneous fibrous structure of the generated electrospun scaffolds. For the drug-loaded scaffolds, a significant increase in the fiber diameters could be observed. This may be due to the increase in viscosity of the electrospun solution and also the presence of the drug molecules within the polymeric fibers [54]. The mean values of the fiber diameter remained still lower than 200 nm, and a regular fibrous structure with no beads was maintained. The increased fiber diameters after drug encapsulation did not affect the mechanical properties such as the Young's modulus or the tensile strength of the electrospun scaffold. Soliman et al. [55] and Milleret et al. [56] showed in previous studies that fiber diameter and orientation, as well as scaffold porosity can impact the mechanical properties of the scaffolds. In particular, they both proved that an increase in the fiber diameter leads to a significant increase in the Young's modulus [55,56]. However, they analyzed differences in the diameter values that were in the μm range [55,56]. In our work, the variation in the fiber diameters is probably too low to significantly impact the investigated mechanical properties. By adding DCF-Gly, the wettability of the scaffolds was also not affected. The scaffolds remained highly hydrophobic as it is described for pure PLA [26]. We have chosen PLA as the drug carrier, since hydrophobicity is important to ensure the drug diffusion from the scaffold into the lesion [57,58].

DCF-Gly encapsulation could be easily visualized using MPM due to the ability to selectively induce DCF autofluorescence [59]. One of the advantages of the MPM technique is the ability to image non-invasively and thus without destroying or modifying the samples [60,61]. This enables a simple, in situ quality control. MPM has already been used to image scaffolds with and without a fibrous structure [62,63]; however, a good contrast or resolution could not be achieved so far. Interestingly, we obtained a good contrast using a very low laser power (3.2 mW). This approach is promising and could be potentially extended to different substrates since a great number of drugs and endogenous molecules are autofluorescent when excited at defined wavelengths. Here, we used MPM to show successful encapsulation and release of the prodrug. By calculating the GVI, it was possible to estimate the amount of non-released DCF-Gly. After 24 h, 10% of DCF-Gly remained in the scaffold, which is comparable to values from literature described by Sidney et al. for previously developed DCF eluting systems [43]. However, the initial burst release was ~60% [43], and in our study only ~20%. Initial burst of drug release is related to drug type, drug concentration, polymer hydrophobicity and to the scaffold nanostructure [64–66]. In contrast to the previously described eluting system, the one described in this study utilized a fibrous structure since it was obtained via electrospinning. Moreover, hydrophobic PLA was used as the only polymer while Sidney et al. used a mixture of the hydrophobic polyesther PLGA (poly-D,L-lactic acid-co-glycolic acid)with the more hydrophilic PEG (poly-ethylene glycol) [43]. In addition, the synthesized DCF-Gly prodrug was used as free acid instead of the Diclofenac sodium salt DCFONa. Carboxylic acids have a lower water solubility than the correspondent sodium salts thus showing a slower and more controlled diffusion over the time [67]. Due to these features, the formulation that is proposed here helps to reduce the initial burst release and to have a sustained drug release from the scaffold over the first 24 h. Furthermore, we investigated the amount of the released drug in the supernatant. It has been shown before, that drug release can be controlled and influenced by changing various parameters such as hydrophobicity, fiber size or drug concentration [68]. In our system, the encapsulated DCF-Gly was effectively released from the scaffold following a controlled Fickian diffusion according to the spectrophotometric measurements and the Peppas equation. This equation has already been employed as a simple model to investigate the drug release from electrospun scaffolds [69,70]. For the here characterized scaffold, the release mechanism undergoes a Fickian diffusion due to a very low diffusion coefficient of 0.29. The encapsulated drug is mostly (~90%) released within the first

Please cite this article in press as: G. Piccirillo et al., Electrospun poly-L-lactide scaffold for the controlled and targeted delivery of a synthetically obtained Diclofenac prodrug to treat actinic keratosis, Acta Biomater. (2016), http://dx.doi.org/10.1016/j.actbio.2016.11.002

24 h. Such a behavior is suitable for the aim of this work considering that DCF is used as a daily treatment to cure AKs [10]. Furthermore, the in vitro biocompatibility of the drug-containing scaffold was tested by performing a MTS cell proliferation assay. This test allows for a quantitative evaluation of cytotoxicity [71] and satisfies the international standard (ISO 10993-5). In contrast to DCFONa, DCF-Gly is non-cytotoxic. It is well known that DCF induces cell death [31,72], suggesting that the newly synthesized molecule is a promising non-cytotoxic prodrug for treating AK. In addition, we investigated the effect of DCF on HDFs after its release from the PLA scaffold employing MPM coupled with FLIM. For the analysis NAD(P)H was chosen as a target [29]. This approach allows the monitoring of changes in cell morphology and metabolism without the need of staining or the interruption of cell culture. The MPM analysis allowed us to image morphological changes in HDFs after the DCF treatment. It is known that DCF induces cell death due to a mitochondrial injury [72]. Specifically, either apoptosis or necrosis is induced depending on how many mitochondria are affected [31]. In this work we aimed to correlate the observed morphological changes to the induced cell death as previously described by Seidenari et al. [32]. In particular, cells that showed a nuclear and cytoplasmic condensation were assessed as apoptotic while cells showing both swelling and vacuolation of the cytoplasm were considered to undergo necrosis [32]. According to the morphological observations obtained with MPM, we suggest that both apoptotic and necrotic events occur after the DCF treatment. FLIM allowed the marker-free detection of the metabolic changes after the DCF treatment. In particular, a significant decrease in the rate of glycolytic NAD(P)H [29] could be detected. Our FLIM data supported the results obtained from the MTS assays.

Our data show that employing a drug-loaded PLA scaffold as a drug-releasing wound dressing to treat AKs could be a very useful and promising alternative to current treatment strategies. It would help to control the daily dosage, thus significantly reducing side-effects, and be applicable as targeted therapy. In addition, the here proposed formulation could be very useful after surgical procedures, photodynamic- and cryotherapy because it would ensure a protection of the treated area and favor the wound healing [73–75]. It has been reported that the application of drug-free electrospun PLA nanofibrous scaffolds as wound dressing materials already enhance the recovery process [76–78], indicating that the here presented combination of PLA and DCF-Gly is a highly interesting candidate for AK treatment. To further improve the functional performance of DCF-Gly, the usage of coaxial and tri-axial electrospinning might be favorable [79,80]. Although this study introduces a potential beneficial system, the effectiveness to treat AK needs to be further investigated in adequate in vivo models. In order to confirm an enhanced transdermal delivery of the synthesized DCF-Gly prodrug compared to DCF [81], further experiments are necessary.

5. Conclusions

In this study, an electrospun PLA scaffold loaded with a synthetically obtained DCF prodrug was generated and characterized. The proposed DCF-Gly synthesis based on the use of SPPS is novel and promising. Compared to non-modified DCF, DCF-Gly is non-cytotoxic and therefore potentially a more suitable drug to treat AK. The electrospun PLA + DCF-Gly scaffold represents an interesting drug releasing system that enables a controlled and targeted delivery of DCF-Gly for the topical treatment of AKs.

Disclosure

None.

Acknowledgements

The authors thank Pirmin Lakner, Daniel A. Carvajal Berrio and Jonas Lindau (University Women's Hospital Tübingen, Germany) for their technical support. Special thanks are due to Shannon L. Layland (Fraunhofer IGB Stuttgart, Germany) for his helpful comments. The authors are grateful for the financial support by the DAAD (Year scholarship program 57130104 to GP), the Fraunhofer-Gesellschaft Internal program (TALENTA 601403 to SH), the Deutsche Forschungsgemeinschaft (INST 2388/30-1) and the Ministry of Science, Research and Arts of Baden Württemberg (Az.: SI-BW 01222-91, 33-729.55-3/214) (both to KS-L).

Appendix A. Supplementary data

Supplementary data associated with this article can be found, in the online version, at http://dx.doi.org/10.1016/j.actbio.2016.11.002.

References

[1] P. Chetty, F. Choi, T. Mitchell, Primary care review of actinic keratosis and its therapeutic options: a global perspective, Dermatol. Ther. 5 (2015) 19–35, http://dx.doi.org/10.1007/s13555-015-0070-9.
[2] T. Oppel, H.C. Korting, Actinic keratosis: the key event in the evolution from photoaged skin to squamous cell carcinoma, Skin Pharmacol. Physiol. 17 (2004) 67–76, http://dx.doi.org/10.1159/000076016.
[3] A.D. Widgerow, S.G. Fabi, R.F. Palestine, A. Rivkin, A. Ortiz, V.W. Bucay, A. Chiu, L. Naga, J. Emer, P.E. Chasan, Extracellular matrix modulation: optimizing skin care and rejuvenation procedures, J. Drugs Dermatol. 15 (2016) s63–s71.
[4] M.J. Sherratt, Tissue elasticity and the ageing elastic fibre, Age 31 (2009) 305–325, http://dx.doi.org/10.1007/s11357-009-9103-6.
[5] P. Lu, K. Takai, V.M. Weaver, Z. Werb, Extracellular matrix degradation and remodeling in development and disease, Cold Spring Harbor perspect. Biol. 3 (2011) 1–24, http://dx.doi.org/10.1101/cshperspect.a005058.
[6] E. Brauchle, H. Johannsen, S. Nolan, S. Thude, K. Schenke-Layland, Design and analysis of a squamous cell carcinoma in vitro model system, Biomaterials 34 (2013) 7401–7407, http://dx.doi.org/10.1016/j.biomaterials.2013.06.016.
[7] S.K. Hussain, J. Sundquist, K. Hemminki, Incidence trends of squamous cell and rare skin cancers in the swedish national cancer registry point to calendar year and age-dependent increases, J. Investig. Dermatol. 130 (2010) 1323–1328, http://dx.doi.org/10.1038/jid.2009.426.
[8] W.D. Tutrone, R. Saini, S. Caglar, J.M. Weinberg, J. Crespo, Topical therapy for actinic keratoses, I: 5-fluorouracil and imiquimod, Cutis 71 (2003) 365–370.
[9] W.D. Tutrone, R. Saini, S. Caglar, J.M. Weinberg, J. Crespo, Topical therapy for actinic keratoses, II: Diclofenac, colchicine, and retinoids, Cutis 71 (2003) 373–379.
[10] C.G. Nelson, Diclofenac gel in the treatment of actinic keratosis, Ther. Clin. Risk Manag. 7 (2011) 207–211, http://dx.doi.org/10.2147/TCRM.S12498.
[11] R.F. Borne, Nonsteroidal anti-inflammatory agents, in: A.D. Williams, L.T. Lemke (Eds.), Foye's Principle of Medicinal Chemistry, 7th ed., Lippincot William and Wilkins, 2013, pp. 1009–1010.
[12] A. Maltusch, J. Röwert-Huber, C. Matthies, S. Lange-Asschenfeldt, E. Stockfleth, Modes of action of diclofenac 3%/hyaluronic acid 2.5% in the treatment of actinic keratosis, J. Deutschen Dermatol. Gesellschaft 9 (2011) 1011–1017, http://dx.doi.org/10.1111/j.1610-0387.2011.07700.x.
[13] L.F. Fecker, E. Stockfleth, I. Nindl, C. Ulrich, T. Forschner, J. Eberle, The role of apoptosis in therapy and prophylaxis of epithelial tumors by nonsteroidal anti-inflammatory drugs (NSAIDs), Br. J. Dermatol. 156 (2007) 25–33, http://dx.doi.org/10.1111/j.1365-2133.2007.07856.x.
[14] A. Naik, Y.N. Kalia, R.H. Guy, Transdermal drug delivery: overcoming the skin's barrier function, Pharm. Sci. Technol. Today 3 (2000) 318–326.
[15] D.C. Peters, R.H. Foster, Diclofenac/hyaluronic acid, Drugs Aging 14 (1999) 313–319.
[16] F. Groeber, M. Holeiter, M. Hampel, S. Hinderer, K. Schenke-Layland, Skin tissue engineering – in vivo and in vitro applications, Adv. Drug Deliv. Rev. 63 (2011) 352–366, http://dx.doi.org/10.1016/j.addr.2011.01.005.
[17] S. Hinderer, E. Brauchle, K. Schenke-Layland, Generation and assessment of functional biomaterial scaffolds for applications in cardiovascular tissue engineering and regenerative medicine, Adv. Healthc. Mater. 4 (2015) 2326–2341, http://dx.doi.org/10.1002/adhm.201400762.
[18] T.J. Sill, A. Horst, Electrospinning: applications in drug delivery and tissue engineering, Biomaterials 29 (2008) 1989–2006, http://dx.doi.org/10.1016/j.biomaterials.2008.01.011.
[19] S.G. Kumbar, P. Syam, S.P. Nukavarapu, R. James, L.S. Nair, C.T. Laurencin, Electrospunpoly(lactic acid-co-glycolic acid) scaffolds for skin tissue engineering, Biomaterials 29 (2008) 4100–4107, http://dx.doi.org/10.1016/j.biomaterials.2008.06.028.

Please cite this article in press as: G. Piccirillo et al., Electrospun poly-L-lactide scaffold for the controlled and targeted delivery of a synthetically obtained Diclofenac prodrug to treat actinic keratosis, Acta Biomater. (2016), http://dx.doi.org/10.1016/j.actbio.2016.11.002

[20] N.A. Weir, F.J. Buchanan, J.F. Orr, G.R. Dickson, Degradation of poly-L-lactide. Part 1: in vitro and in vivo physiological temperature degradation, Proc Inst Mech Eng H 218 (2004) 307–319, http://dx.doi.org/10.1243/0954411041932782.
[21] V.B. Oza, C. Smith, P. Raman, E.K. Koepf, H.A. Lashuel, H.M. Petrassi, K.P. Chiang, E.T. Powers, J. Sachettinni, J.W. Kelly, Synthesis, structure, and activity of Diclofenac analogues as transthyretin amyloid fibril formation inhibitors, J. Med. Chem. 45 (2002) 321–332, http://dx.doi.org/10.1021/jm010257n.
[22] D.J. States, R.A. Haberkorn, D.J. Ruben, A two-dimensional nuclear overhauser experiment with pure absorption phase in four quadrants, J. Magn. Reson. 48 (1969) 286–292, http://dx.doi.org/10.1016/0022-2364(82)90279-7.
[23] NMR Spectroscopy User Guide, Varian NMR Systems, Pub. No. 01-999343-00, Rev. B 1207 (2007).
[24] N.A. Peppas, J. Sahlin, A simple equation for the description of solute release. III. Coupling of diffusion and relaxation, Int. J. Pharm. 57 (1989) 169–172, http://dx.doi.org/10.1016/0378-5173(89)90306-2.
[25] S. Dash, P.N. Murthy, L. Nath, P. Chowdhury, Kinetic modelling on drug release from controlled drug delivery systems, Acta Pol. Pharm. 67 (2010) 217–223.
[26] S. Hinderer, J. Seifert, M. Votteler, N. Shen, J. Rheinlaender, T.E. Schäffer, K. Schenke-Layland, Engineering of a bio-functionalized hybrid off-the-shelf heart valve, Biomaterials 35 (2014) 2130–2139, http://dx.doi.org/10.1016/j.biomaterials.2013.10.080.
[27] M. Pudlas, S. Koch, C. Bolwien, S. Thude, N. Jenne, T. Hirth, H. Walles, K. Schenke-Layland, Tissue Eng. C Methods 17 (2011) 1027–1040, http://dx.doi.org/10.1089/ten.tec.2011.0082.
[28] R. Albulescu, E. Codorean, L. Albulescu, G. Caraene, V. Vulturescu, C. Tanase, In vitro biocompatibility testing of implantable biomaterials, Romanian Biotechnol. Lett. 13 (2008) 3863–3872.
[29] T.G. Scott, R.D. Spencer, N.J. Leonard, G. Weber, Synthetic spectroscopic models related to coenzymes and base pairs. V. Emission properties of NADH. Studies of fluorescence lifetimes and quantum efficiencies of NADH, AcPyADH, [reduced acetylpyridineadenine dinucleotide] and simplified synthetic models, J. Am. Chem. Soc. 92 (1970) 687–695, http://dx.doi.org/10.1021/ja00706a043.
[30] W. Li, J. Zhou, Y. Xu, Study of the in vitro cytotoxicity testing of medical devices, Biomed. Rep. 3 (2015) 617–620, http://dx.doi.org/10.3892/br.2015.481.
[31] U.A. Boelsterli, Diclofenac-induced liver injury: a paradigm of idiosyncratic drug toxicity, Toxicol. Appl. Pharmacol. 192 (2003) 307–322, http://dx.doi.org/10.1016/S0041-008X(03)00368-5.
[32] S. Seidenari, S. Schianchi, P. Azzoni, L. Benassi, S. Borsari, J. Cautela, C. Ferrari, P. French, S. Giudice, K. Koenig, C. Magnoni, C. Talbot, C. Dunsby, High-resolution multiphoton tomography and fluorescence lifetime imaging of UVB-induced cellular damage on cultured fibroblasts producing fibres, Skin Res. Technol. 19 (2013) 251–257, http://dx.doi.org/10.1111/srt.12034.
[33] D. Liang, B.S. Hsiao, B. Chu, Functional electrospun nanofibrous scaffolds for biomedical applications, Adv. Drug Deliv. Rev. 59 (2007) 1392–1412, http://dx.doi.org/10.1016/j.addr.2007.04.021.
[34] T. Garg, O. Singh, S. Arora, R. Murthy, Scaffold: a novel carrier for cell and drug delivery, Crit. Rev. Ther. Drug Carrier Syst. 29 (2012) 1–63, http://dx.doi.org/10.1615/Crit.Rev.Ther.DrugCarrierSyst.v29.i1.10.
[35] R.E. Drumright, P.R. Gruber, D.E. Henton, Polylactic acid technology, Adv. Mater. 12 (2000) 1841–1846, http://dx.doi.org/10.1002/1521-4095(200012)12:23∗1841.
[36] S. Honarbakhsh, B. Pourdeyhimi, Scaffolds for drug delivery, part I: electrospun porous poly(lactic acid) and poly(lactic acid)/poly(ethylene oxide) hybrid scaffolds, J. Mater. Sci. 46 (2010) 2874–2881, http://dx.doi.org/10.1007/s10853-010-5161-5.
[37] S. Bushuven, D. Heise, J. Bolbrinker, Diclofenac update – Part 1: pharmacology and comparison with other drugs, Anasthesiol. Intensivmed. Notfallmed. Schmerzther. 49 (2014) 588–598, http://dx.doi.org/10.1055/s-0034-1395170.
[38] S. Bushuven, D. Heise, J. Bolbrinker, Diclofenac update – Part 2: pharmacology and comparison with other drugs, Anasthesiol. Intensivmed. Notfallmed. Schmerzther. 49 (2014) 670–680, http://dx.doi.org/10.1055/s-0040-100121.
[39] J. Zacher, R. Altman, N. Bellamy, P. Brühlmann, J. Da Silva, E. Huskisson, R.S. Taylor, Topical diclofenac and its role in pain and inflammation: an evidence-based review, Curr. Med. Res. Opin. 24 (2008) 925–950, http://dx.doi.org/10.1185/030079908X273066.
[40] H.F. Merk, Topical diclofenac in the treatment of actinic keratoses, Int. J. Dermatol. 46 (2007) 12–18, http://dx.doi.org/10.1111/j.1365-4632.2007.03060.x.
[41] R. Altman, B. Bosch, K. Brune, P. Patrignani, C. Young, Advances in NSAID Development: Evolution of Diclofenac Products Using, Pharm. Technol. 75 (2015) 859–877, http://dx.doi.org/10.1007/s40265-015-0392-z.
[42] M. Brunner, P. Dehghanyar, B. Seigfried, W. Martin, G. Menke, M. Müller, Favourable dermal penetration of diclofenac after administration to the skin using a novel spray gel formulation, Br. J. Clin. Pharmacol. 60 (2005) 573–577, http://dx.doi.org/10.1111/j.1365-2125.2005.02484.x.
[43] L.E. Sidney, T.R. Heathman, E.R. Britchford, A. Abed, C.V. Rahman, L.D. Buttery, Investigation of localized delivery of diclofenac sodium from poly (D,L-lactic acid-co-glycolic acid)/ poly (ethylene glycol) scaffolds using an in vitro osteoblast inflammation model, Tissue Eng. Part A 21 (2015) 362–373, http://dx.doi.org/10.1089/ten.tea.2014.0100.
[44] L. Tammaro, G. Russo, V. Vittoria, Encapsulation of Diclofenac molecules into poly (-caprolactone) electrospun fibers for delivery protection, J. Nanomater. (2009), http://dx.doi.org/10.1155/2009/238206. Article ID 238206 8 pages.
[45] R.O. Gaitano, N.L. Calvo, G.E. Narda, T.S. Kaufman, R.M. Maggio, E.V. Brusau, Preparation and physical characterization of a Diclofenac-ranitidine co-precipitate for improving the dissolution of Diclofenac, J. Pharm. Sci. 105 (2016) 1258–1268, http://dx.doi.org/10.1016/j.xphs.2016.01.001.
[46] K.M. Huttunen, H. Raunio, J. Rautio, Prodrugs—from serendipity to rational design, Pharmacol. Rev. 63 (2011) 750–771, http://dx.doi.org/10.1124/pr.110.003459.
[47] Y. Yang, H. Aloysius, D. Inoyama, Y. Chen, L. Hu, Enzyme-mediated hydrolytic activation of prodrugs, Acta Pharmaceut. Sin. B 1 (2011) 143–159, http://dx.doi.org/10.1016/j.apsb.2011.08.001.
[48] R. Behrendt, P. White, J. Offer, Advances in Fmoc solid-phase peptide synthesis, J. Pept. Sci. 22 (2016) 4–27, http://dx.doi.org/10.1002/psc.2836.
[49] S. Kumar, D.K. Tyagi, A. Gupta, Synthesis and evaluation of amide prodrugs of diclofenac, J. Pharm. Sci. Res. 2 (2010) 369–375.
[50] W.J. Hoekstra, The 2-chlorotrityl resin: a worthy addition to the medicinal chemist's toolbox, Curr. Med. Chem. 8 (2001) 715–719, http://dx.doi.org/10.2174/0929867013373192.
[51] R. Bollhagen, M. Schmiedberger, K. Barlos, E. Grell, A new reagent for the cleavage of fully protected peptides synthesized on 2-chlorotrityl chloride resin, Chem. Soc. Chem. Commun. 22 (1994) 2559–2560, http://dx.doi.org/10.1039/C39940002559R.
[52] K. Barlos, O. Chatzi, D. Gatos, G.K. Stavropoulos, 2-chlorotrityl chloride resin — studies on anchoring of Fmoc-amino acids and peptide cleavage, Int. J. Peptide Protein Res. 37 (1991) 513–520, http://dx.doi.org/10.1111/j.1399-3011.1991.tb00769.x.
[53] M.P. Gashti, F. Alimohammadi, J. Hulliger, M. Burgener, H. Oulevey-Aboulfad, G.L. Bowlin, Current microscopy contributions to advances, Sci. Technol. 1 (2012) 625–638.
[54] S.Y. Chew, T.C. Hufnagel, C.T. Lim, K.W. Leong, Mechanical properties of single electrospun drug-encapsulated nanofibers, Nanotechnology 17 (2006) 3880–3891, http://dx.doi.org/10.1088/0957-4484/17/15/045.
[55] S. Soliman, S. Sant, J.W. Nichol, M. Khabiry, E. Traversa, A. Khademhosseini, Controlling the porosity of fibrous scaffolds by modulating the fiber diameter and packing density, J. Biomed. Mater. Res. 96A (2011) 566–574, http://dx.doi.org/10.1002/jbm.a.33010.
[56] V. Milleret, S. Benjamin, P. Neuenschwander, H. Hall, Tuning electrospinning parameters for production of 3D-fiber-fleeces with increased porosity for soft tissue engineering applications, Eur. Cell Mater. 22 (2011) 286–303.
[57] L. Kesong, X. Yaob, L. Jiang, Recent developments in bio-inspired special wettability, Chem. Soc. Rev. 39 (2010) 3240–3255, http://dx.doi.org/10.1039/B917112F.
[58] A. Marmur, Super-hydrophobicity fundamentals: implications to biofouling prevention, Biofouling J. Bioadhes. Biofilm Res. 22 (2006) 107–115, http://dx.doi.org/10.1080/08927010600562328.
[59] W. Baeyens, G. Van Der Weken, M. Schelkens, Diclofenac and naproxen analysis by microbore liquid chromatography (LC) with native fluorescence detection, J. Fluorescence 5 (1995) 131–134, http://dx.doi.org/10.1007/BF00727529.
[60] K. König, K. Schenke-Layland, I. Riemann, U.A. Stock, Multiphoton autofluorescence imaging of intratissue elastic fibers, Biomaterials 26 (2005) 495–500, http://dx.doi.org/10.1016/j.biomaterials.2004.02.059.
[61] K. Schenke-Layland, Non-invasive multiphoton imaging of extracellular matrix structures, J. Biophotonics 1 (2008) 451–462, http://dx.doi.org/10.1002/jbio.200810045.
[62] M. Vielreicher, S. Schürmann, R. Detsch, M.A. Schmidt, A. Buttgereit, A. Boccaccini, O. Friedrich, Taking a deep look: modern microscopy technologies to optimize the design and functionality of biocompatible scaffolds for tissue engineering in regenerative medicine, J. R. Soc. Interface 10 (2013) 1–21, http://dx.doi.org/10.1098/rsif.2013.0263.
[63] Y. Sun, H.Y. Tan, S.J. Lin, H.S. Lee, T.Y. Lin, S.H. Jee, T.H. Young, W. Lo, W.L. Chen, C.Y. Dong, Imaging tissue engineering scaffolds using multiphoton microscopy, Microsc. Res. Technol. 71 (2008) 140–145, http://dx.doi.org/10.1002/jemt.20537.
[64] H.K. Makadia, S.J. Siegel, Poly lactic-co-glycolic acid (PLGA) as biodegradable controlled drug delivery carrier, Polymers 3 (2011) 1377–1397, http://dx.doi.org/10.3390/polym3031377.
[65] V. Pillay, C. Dott, Y.E. Choonara, C. Tyagi, L. Tomar, P. Kumar, L.C. du Toit, V.M.K. Ndesendo, A review of the effect of processing variables on the fabrication of electrospun nanofibers for drug delivery applications, J. Nanomater. (2013) 1–22, http://dx.doi.org/10.1155/2013/789289.
[66] A. Haider, S. Haider, I. Kang, A comprehensive review summarizing the effect of electrospinning parameters and potential applications of nanofibers in biomedical and biotechnology, Arab. J. Chem. 12 (2015) 1878–5352, http://dx.doi.org/10.1016/j.arabjc.2015.11.015.
[67] D.C. Coughlan, O.I. Corrigan, Release kinetics of benzoic acid and its sodium salt from a series of poly(n-isopropylacrylamide) matrices with various percentage, J. Pharm. Sci. 97 (2008) 318–330, http://dx.doi.org/10.1002/jps.21095.
[68] L. Liu, S. Bai, H. Yang, S. Li, J. Quan, L. Zhu, H. Nie, Controlled release from thermo-sensitive PNVCL-co-MAA electrospun nanofibers: the effects of hydrophilicity/ hydrophobicity of a drug, Mater. Sci. Eng. C Mater. Biol. Appl. 67 (2016) 581–589, http://dx.doi.org/10.1016/j.msec.2016.05.083.
[69] M. Maleki, M. Amani-Tehran, M. Latifi, S. Mathur, Drug release profile in core–shell nanofibrous structures: a study on Peppas equation and artificial neural network modeling, Comput. Methods Programs Biomed. 113 (2014) 92–100, http://dx.doi.org/10.1016/j.cmpb.2013.09.003.

Please cite this article in press as: G. Piccirillo et al., Electrospun poly-L-lactide scaffold for the controlled and targeted delivery of a synthetically obtained Diclofenac prodrug to treat actinic keratosis, Acta Biomater. (2016), http://dx.doi.org/10.1016/j.actbio.2016.11.002

[70] A. Repanas, B. Glasmacher, Dipyridamole embedded in polycaprolactone fibers prepared by coaxial electrospinning as a novel drug delivery system, J. Drug Deliv. Sci. Technol. 29 (2015) 132–142, http://dx.doi.org/10.1016/j.jddst.2015.07.001.
[71] A.H. Cory, T.C. Owen, J.A. Barltrop, J.G. Cory, Use of an aqueous soluble tetrazolium/formazan assay for cell growth assays in culture, Cancer Commun. 3 (1991) 207–212.
[72] R. Bort, X. Ponsoda, R. Jover, M.J. Gómez-Lechón, J.V. Castell, Diclofenac toxicity to hepatocytes: a role for drug metabolism in cell toxicity, J. Pharmacol. Exp. Ther. 288 (1999) 65–72.
[73] E.E. Uhlenhake, Optimal treatment of actinic keratosis, Clin. Interv. Aging 8 (2013) 29–35, http://dx.doi.org/10.2147/CIA.S31930.
[74] J.M. Berlin, D.S. Rigel, Diclofenac sodium 3% gel in the treatment of actinic keratosis postcryosurgery, J. Drugs Dermatol. 7 (2008) 669–673.
[75] J. Jorizzo, J. Weiss, K. Furst, C. VandePol, S.F. Levy, Effect of a 1-week treatment with 0.5% topical fluorouracil on occurrence of actinic keratosis after cryosurgery: a randomized, vehicle-controlled clinical trial, Arch. Dermatol. 140 (2004) 813–816, http://dx.doi.org/10.1001/archderm.140.7.813.
[76] J. Venugopal, S. Ramakrishna, Applications of polymer nanofibers in biomedicine and biotechnology, Appl. Biochem. Biotechnol. 125 (2005) 147–158, http://dx.doi.org/10.1385/ABAB:125:3:147.
[77] P. Zahedi, I. Rezaeian, S.O. Ranaei-Siadat, S.H. Jafari, P. Supaphol, A review on wound dressings with an emphasis on electrospun nanofibrous polymeric bandages, Polym. Adv. Technol. 21 (2010) 77–95, http://dx.doi.org/10.1002/pat.1625.
[78] A. Toncheva, M. Spasova, D. Paneva, N. Manolova, I. Rashkov, Polylactide (PLA)-based electrospun fibrous materials containing ionic drugs as wound dressing materials: a review, Int. J. Polym. Mater. Polym. Biomater. 63 (2014) 657–667, http://dx.doi.org/10.1080/00914037.2013.854240.
[79] C. Yang, D. Yu, D. Pan, X. Liu, X. Wang, S.W. Annie Bligh, G.R. Williams, Electrospun pH-sensitive core–shell polymer nanocomposites fabricated using a tri-axial process, Acta Biomater. 35 (2016) 77–86, http://dx.doi.org/10.1016/j.actabio.2016.029.029.
[80] H. Wen, C. Yang, D. Yu, X. Li, D. Zhang, Electrospun zein nanoribbons for treatment of lead-contained wastewater, Chem. Eng. J. 290 (2016) 263–272, http://dx.doi.org/10.1016/j.cej.2016.01.055.
[81] S. Lobo, H. Li, N. Farhan, G. Yan, Evaluation of diclofenac prodrugs for enhancing transdermal delivery, Drug Dev. Ind. Pharm. 40 (2014) 425–432, http://dx.doi.org/10.3109/03639045.2013.767828.

Please cite this article in press as: G. Piccirillo et al., Electrospun poly-L-lactide scaffold for the controlled and targeted delivery of a synthetically obtained Diclofenac prodrug to treat actinic keratosis, Acta Biomater. (2016), http://dx.doi.org/10.1016/j.actbio.2016.11.002